

## Diels–Alder Exo Selectivity in Terminal-Substituted Dienes and Dienophiles: Experimental Discoveries and Computational Explanations

Yu-hong Lam,<sup>†</sup> Paul Ha-Yeon Cheong,<sup>‡</sup> José M. Blasco Mata,<sup>†</sup> Steven J. Stanway,<sup>§</sup> Véronique Gouverneur,<sup>\*,†</sup> and K. N. Houk<sup>\*,‡</sup>

Chemistry Research Laboratory, University of Oxford, U.K., Department of Chemistry and Biochemistry, University of California, Los Angeles, California 90095, and Neurology and GI Centre of Excellence for Drug Discovery, GlaxoSmithKline, Harlow, Essex, U.K.

Received October 8, 2008; E-mail: veronique.gouverneur@chem.ox.ac.uk; houk@chem.ucla.edu

**Abstract:** The Diels–Alder reactions of a series of silyloxydienes and silylated dienes with acyclic  $\alpha,\beta$ -unsaturated ketones and *N*-acyloxazolidinones have been investigated. The endo/exo stereochemical outcome is strongly influenced by the substitution pattern of the reactants. High exo selectivity was observed when the termini of the diene and the dienophile involved in the shorter of the forming bonds were both substituted, while the normal endo preference was found otherwise. The exo-selective asymmetric Diels–Alder reactions using Evans' oxazolidinone chiral auxiliary furnished a high level of  $\pi$ -facial selectivity in the same sense as their well-documented endo-selective counterparts. Computational results for these Diels–Alder reactions were consistent with the experimental endo/exo selectivity in most cases. A twist-asynchronous model accounts for the geometries and energies of the computed transition structures.

### Introduction

Precise control of stereoselectivity in the installation of asymmetric centers constitutes a prominent goal in organic synthesis. The Diels–Alder reaction is indispensable for the stereoselective construction of six-membered rings,<sup>1</sup> a structural motif widely found in natural products. In its intermolecular variant, a cyclohexene ring with up to four stereocenters can be formed in a single step from acyclic precursors, often with high levels of regio- and stereocontrol. A familiar property of this reaction, whether thermal or catalyzed, is its endo diastereoselectivity.<sup>2</sup> As a result, the formation of these stereogenic centers on the ring is often regarded as “predictable in a relative sense”.<sup>3</sup>

In contrast, instances of the Diels–Alder reaction showing exo selectivity occur less frequently, at least in an intermolecular context. Apart from some isolated cases,<sup>4,5</sup> certain structural motifs on the dienophile are well-known to lead predominantly to exo cycloadducts, including conformationally restricted cyclic *s-cis* dienophiles<sup>6</sup> and  $\alpha$ -halo  $\alpha,\beta$ -unsaturated carbonyl compounds.<sup>7</sup>

Synthetic protocols geared toward an exo-selective Diels–Alder reaction usually entail the use of structurally elaborate starting

materials that incorporate strategic design features. These features are often anticipated to sterically encumber the endo mode of approach of the reactants (Scheme 1). Danishefsky and co-workers<sup>8</sup> utilized a *gem*-dimethyl group and a bulky aroyl group on the diene and dienophile, respectively, to divert the cycloaddition into the desired exo manifold by virtue of their steric bulk. This was applied in the total synthesis of racemic maminuthaquinone (eq 1 in Scheme 1).

- (4) (a) Sammis, G. M.; Flamme, E. M.; Xie, H.; Ho, D. M.; Sorensen, E. J. *J. Am. Chem. Soc.* **2005**, *127*, 8612. (b) Pritchard, R. G.; Stoodley, R. J.; Yuen, W.-H. *Org. Biomol. Chem.* **2005**, *3*, 162. (c) Pellegrinet, S. C.; Spanevello, R. A. *Org. Lett.* **2000**, *2*, 1073. (d) Kozmin, S. A.; Rawal, V. H. *J. Org. Chem.* **1997**, *62*, 5252. (e) Fraile, J. M.; García, J. I.; Gracia, D.; Mayoral, J. A.; Pires, E. *J. Org. Chem.* **1996**, *61*, 9479. (f) Node, M.; Nishide, K.; Imazato, H.; Kurosaki, R.; Inoue, T.; Ikariya, T. *Chem. Commun.* **1996**, 2559. (g) Ward, D. E.; Gai, Y. *Tetrahedron Lett.* **1992**, *33*, 1851. (h) Lamy-Schelkens, H.; Giomi, D.; Ghosez, L. *Tetrahedron Lett.* **1989**, *30*, 5887. Exo-selective catalytic asymmetric Diels–Alder reactions of Danishefsky-type dienes and  $\alpha,\beta$ -unsaturated *N*-acyloxazolidinones have also been disclosed very recently. See: (i) Sudo, Y.; Shirasaki, D.; Harada, S.; Nishida, A. *J. Am. Chem. Soc.* **2008**, *130*, 12588. For a report on an exo-selective Diels–Alder reaction that also includes a mechanistic discussion, see: (j) Ge, M.; Stoltz, B. M.; Corey, E. J. *Org. Lett.* **2000**, *2*, 1927.
- (5) Boren, B.; Hirschi, J. S.; Reibenspies, J. H.; Tallant, M. D.; Singleton, D. A.; Sulikowski, G. A. *J. Org. Chem.* **2003**, *68*, 8991.
- (6) (a) Cernak, T. A.; Gleason, J. L. *J. Org. Chem.* **2008**, *73*, 102. (b) Qi, J.; Roush, W. R. *Org. Lett.* **2006**, *8*, 2795. (c) Roush, W. R.; Barda, D. A.; Limberakis, C.; Kunz, R. K. *Tetrahedron* **2002**, *58*, 6433. (d) Takeda, K.; Imaoka, I.; Yoshii, E. *Tetrahedron* **1994**, *50*, 10839. (e) Pyne, S. G.; Safaei-G, J.; Hockless, D. C. R.; Skelton, B. W.; Sobolev, A. N.; White, A. H. *Tetrahedron* **1994**, *50*, 941. (f) Roush, W. R.; Brown, B. B. *J. Org. Chem.* **1992**, *57*, 3380. (g) Adam, W.; Albert, R.; Hasemann, L.; Nava Salgado, V. O.; Nestler, B.; Peters, E.-M.; Peters, K.; Prechtel, F.; von Schnering, H. G. *J. Org. Chem.* **1991**, *56*, 5782.
- (7) Corey, E. J.; Loh, T.-P. *J. Am. Chem. Soc.* **1991**, *113*, 8966.
- (8) Yoon, T.; Danishefsky, S. J.; de Gala, S. *Angew. Chem., Int. Ed. Engl.* **1994**, *33*, 853.

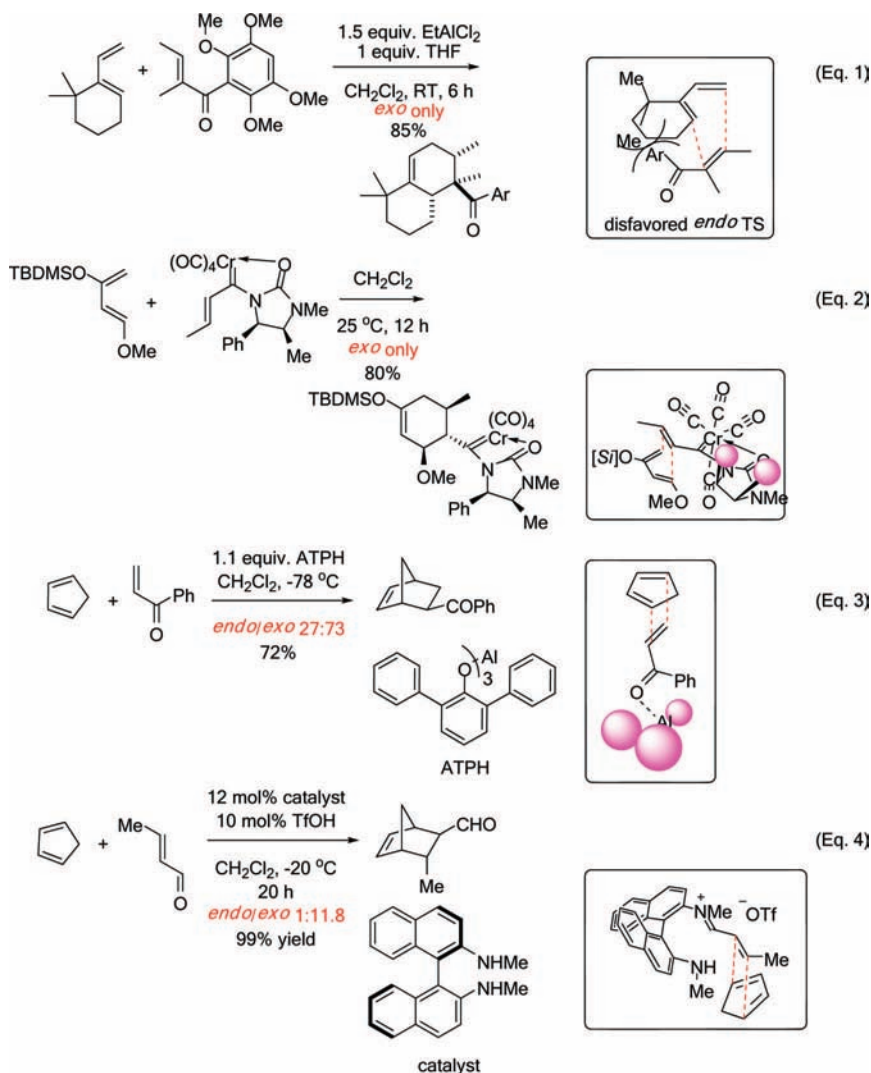
<sup>†</sup> University of Oxford.

<sup>‡</sup> University of California, Los Angeles.

<sup>§</sup> GlaxoSmithKline.

- (1) Fringuelli, F.; Taticchi, A. *The Diels–Alder Reaction: Selected Practical Methods*; Wiley: Chichester, U.K., 2002.
- (2) (a) Carey, F. A.; Sundberg, R. J. *Advanced Organic Chemistry, Part A: Structure and Mechanisms*, 5th ed.; Springer: New York, 2007; pp 834–873. (b) Kürti, L.; Czako, B. *Strategic Applications of Named Reactions in Organic Synthesis*; Elsevier: Burlington, MA, 2005; pp 140–141.
- (3) Nicolaou, K. C.; Snyder, S. A.; Montagnon, T.; Vassilikogiannakis, G. *Angew. Chem., Int. Ed.* **2002**, *41*, 1668.

Scheme 1. Selected Examples of Substrate- and Catalyst-Controlled Exo-Selective Intermolecular Diels–Alder Reactions



Homochiral  $\alpha,\beta$ -unsaturated *N*-acylamino Fischer carbenes containing an oxazolidinone or imidazolidinone moiety have been used as exo-selective dienophiles in cycloadditions of cyclopentadiene and other acyclic dienes.<sup>9</sup> The apically disposed carbonyl ligands on the octahedrally coordinated metal center furnished the steric hindrance for impeding the endo trajectory (eq 2 in Scheme 1). Other stoichiometric organometallic reagents have also been reported to give a high exo selectivity.<sup>10</sup>

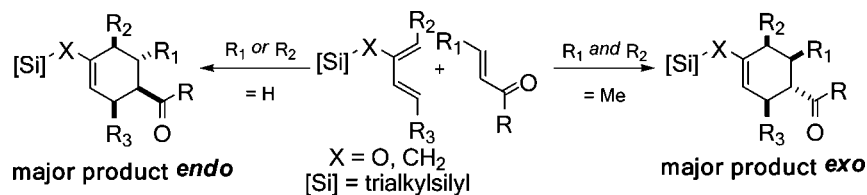
An early example of catalyst-controlled exo-selective Diels–Alder reactions was reported by Yamamoto and co-workers.<sup>11</sup> The bulky Lewis acid aluminum tris(2,6-diphenylphenoxide) was shown to facilitate exo cycloaddition of cyclopentadiene and phenyl vinyl ketone, a pair of reactants that give predominantly an endo cycloadduct otherwise (eq 3

in Scheme 1). Exo-selective cycloadditions of cyclopentadiene or diphenylisobenzofuran and  $\alpha,\beta$ -unsaturated aldehydes were documented by MacMillan and co-workers<sup>12</sup> among the first highly enantioselective organocatalytic Diels–Alder reactions. More recently, Ishihara and Nakano<sup>13</sup> reported the use of a chiral binaphthyl-substituted diamine in cycloadditions using  $\alpha$ -acyloxyacroleins as dienophiles. A structurally related, binaphthyl-based diamine was found by Maruoka and co-workers<sup>14</sup> to be an effective catalyst in the exo-selective cycloadditions with *trans*-cinnamaldehyde and two other  $\alpha,\beta$ -unsaturated aldehydes. The high exo selectivity has been attributed to the steric hindrance of the binaphthyl moiety in the reactive iminium intermediate formed from the dienophile and the catalyst (eq 4 in Scheme 1).<sup>15</sup> Gotoh and Hayashi<sup>16</sup> extended the scope of  $\alpha,\beta$ -unsaturated aldehydes suitable for exo-selective cycloadditions by using a diarylprolinol silyl ether as the organocatalyst. In all of these reports on organocatalyzed Diels–Alder reactions, instances where a high exo-selectivity is observed involve the use of cyclopentadiene as the diene component.

- (9) Powers, T. S.; Jiang, W.; Su, J.; Wulff, W. D.; Waltermire, B. E.; Rheingold, A. L. *J. Am. Chem. Soc.* **1997**, *119*, 6438.  
 (10) (a) Barluenga, J.; Canteli, R.-M.; Flórez, J.; García-Granda, S.; Gutiérrez-Rodríguez, A.; Martín, E. *J. Am. Chem. Soc.* **1998**, *120*, 2514. (b) Richardson, B. M.; Welker, M. E. *J. Org. Chem.* **1997**, *62*, 1299. (c) Wright, M. W.; Smalley, T. L.; Welker, M. E.; Rheingold, A. L. *J. Am. Chem. Soc.* **1994**, *116*, 6777. (d) Sabat, M.; Reynolds, K. A.; Finn, M. G. *Organometallics* **1994**, *13*, 2084. (e) Gilbertson, S. R.; Zhao, X.; Dawson, D. P.; Marshall, K. L. *J. Am. Chem. Soc.* **1993**, *115*, 8517.  
 (11) Maruoka, K.; Imoto, H.; Yamamoto, H. *J. Am. Chem. Soc.* **1994**, *116*, 12115.

- (12) Ahrendt, K. A.; Borths, C. J.; MacMillan, D. W. C. *J. Am. Chem. Soc.* **2000**, *122*, 4243.  
 (13) Ishihara, K.; Nakano, K. *J. Am. Chem. Soc.* **2005**, *127*, 10504.  
 (14) Kano, T.; Tanaka, Y.; Maruoka, K. *Org. Lett.* **2006**, *8*, 2687.  
 (15) Kano, T.; Tanaka, Y.; Maruoka, K. *Chem.–Asian J.* **2007**, *2*, 1161.  
 (16) Gotoh, H.; Hayashi, Y. *Org. Lett.* **2007**, *9*, 2859.

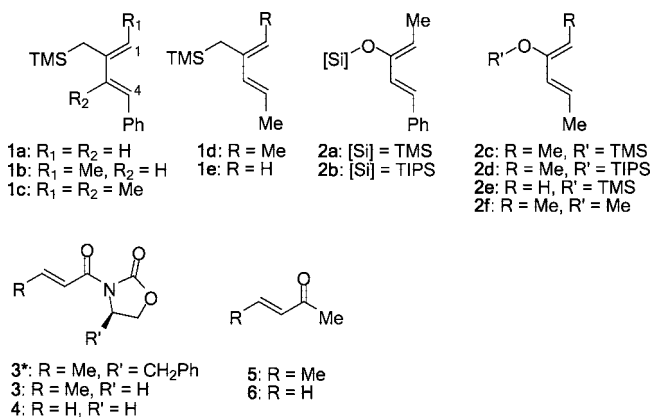
## Scheme 2. Stereochemical Dependence on the Substitution Pattern of the Starting Materials



Examples of exo-selective Diels–Alder reactions are also found in host–guest chemistry. Thus, a trimeric porphyrin host facilitates an exclusively exo cycloaddition of a furan and a maleimide by orienting them in the required disposition.<sup>17</sup> The exo orientation can also be fulfilled by hydrogen bonding within the supramolecular complex.<sup>18</sup> Monoclonal antibodies that catalyze enantioselective Diels–Alder reactions of *N*-acylamino-1,3-butadienes and *N,N*-dimethylacrylamide in an either endo- or exo-specific fashion have also been derived.<sup>19</sup>

During the study of the preparation of enantioenriched fluorinated carbocycles,<sup>20</sup> we synthesized an array of Diels–Alder cycloadducts featuring an allylsilane or a silyl enol ether, starting from all-carbon silylated dienes<sup>21</sup> or silyloxy dienes, respectively (Scheme 2).<sup>22,23</sup> We observed a remarkable change in the endo/exo stereoselectivity of the cycloaddition that depends on the substitution pattern of the starting material. As depicted in Scheme 2, when both R<sub>1</sub> and R<sub>2</sub> are a methyl group (Scheme 2, right), the adducts with four stereocenters are formed with a consistently high exo selectivity. Use of the desmethyl diene and/or dienophile leads to the “normal” endo products predominantly (Scheme 2, left). The observation that such a minor modification of the substituents on these common substrates could lead to a dramatic change in endo/exo selectivity is

Chart 1. Structures of Dienes 1 and 2 and Dienophiles 3–6



intriguing, not least because it holds obvious implications for the stereodefined synthesis of carbocycles in general. We now detail the synthetic results obtained with this class of substituent-dependent, exo-selective Diels–Alder reactions as well as the results of computational studies that reveal the origins of these selectivities.

## Synthetic Results and Discussion

The dienes **1** and **2** and dienophiles **3–6** that form the basis of this work are shown in Chart 1. The silylated dienes and silyloxydienes<sup>24</sup> and the dienophiles<sup>25</sup> were either readily synthesized by reported methods or were commercially available. The numbering of the product cycloadducts is shown in Figure 1.

The Diels–Alder reactions involving the  $\alpha,\beta$ -unsaturated *N*-acyloxazolidinone **3** and their asymmetric variants mediated by Evans' chiral auxiliary **3\***<sup>26</sup> are listed in entries 1–8 of Table 1. These were performed in dichloromethane at  $-40\text{ }^\circ\text{C}$  promoted by 1.4 equiv of Me<sub>2</sub>AlCl. As previously reported,<sup>20</sup> the asymmetric Diels–Alder reaction of silylated diene **1a** with the homochiral **3\*** delivered *endo*-**7** as the major product with complete C <sub>$\alpha$</sub> -*Re* facial selectivity (entry 1).<sup>26</sup> Under otherwise identical conditions, however, diene **1b**, which has an extra methyl group at C1, afforded *exo*-**8** as the sole isolated product (entry 2). As proved by X-ray crystallography of *exo*-**8**, this cycloaddition also arises from attack on the homochiral dienophile at its C <sub>$\alpha$</sub> -*Re* face exclusively. The sense of asymmetric induction in this case is thus identical to that observed in their endo-selective counterparts involving **1a** and other reported dienes.<sup>26</sup> Reaction of diene **1c** bearing an additional methyl group at C3 yielded comparable results (entry 3). The sense of

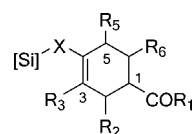
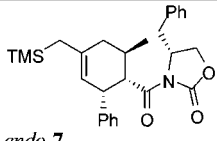
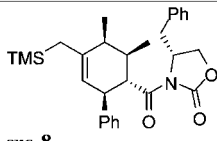
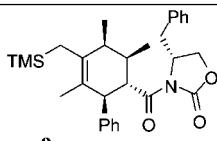
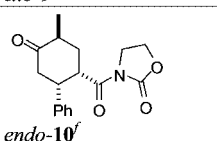
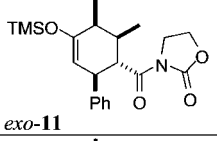
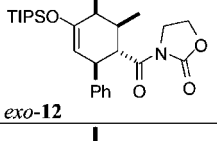
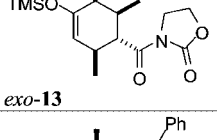
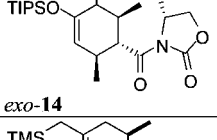
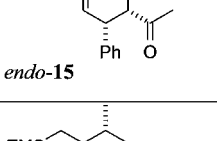
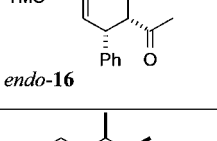
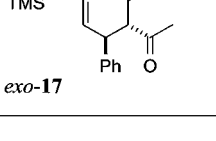


Figure 1. Numbering of cycloadducts.

- (17) Walter, C. J.; Anderson, H. L.; Sanders, J. K. M. *J. Chem. Soc., Chem. Commun.* **1993**, 458.
- (18) Pearson, R. J.; Kassianidis, E.; Philp, D. *Tetrahedron Lett.* **2004**, 45, 4777.
- (19) (a) Cannizzaro, C. E.; Ashley, J. A.; Janda, K. D.; Houk, K. N. *J. Am. Chem. Soc.* **2003**, 125, 2489. (b) Heine, A.; Stura, E. A.; Yli-Kauhaluoma, J. T.; Gao, C.; Deng, Q.; Beno, B. R.; Houk, K. N.; Janda, K. D.; Wilson, I. A. *Science* **1998**, 279, 1934. (c) Yli-Kauhaluoma, J. T.; Ashley, J. A.; Lo, C.-H.; Tucker, L.; Wolfe, M. M.; Janda, K. D. *J. Am. Chem. Soc.* **1995**, 117, 7041. (d) Gouverneur, V. E.; Houk, K. N.; de Pascual-Teresa, B.; Beno, B.; Janda, K. D.; Lerner, R. A. *Science* **1993**, 262, 204.
- (20) Lam, Y.-h.; Bobbio, C.; Cooper, I. R.; Gouverneur, V. *Angew. Chem., Int. Ed.* **2007**, 46, 5106.
- (21) For related Diels–Alder reactions of all-carbon silylated dienes, see: (a) Ryu, D. H.; Corey, E. J. *J. Am. Chem. Soc.* **2003**, 125, 6388. (b) Vedejs, E.; Duncan, S. M. *J. Org. Chem.* **2000**, 65, 6073. (c) Organ, M. G.; Winkle, D. D. *J. Org. Chem.* **1997**, 62, 1881. (d) Corey, E. J.; Letavic, M. A. *J. Am. Chem. Soc.* **1995**, 117, 9616. (e) Krafft, G. A.; Garcia, E. A.; Guram, A.; O'Shaughnessy, B.; Xu, X. *Tetrahedron Lett.* **1986**, 27, 2691. (f) Sakurai, H.; Hosomi, A.; Saito, M.; Sasaki, K.; Iguchi, H.; Sasaki, J.-I.; Araki, Y. *Tetrahedron* **1983**, 39, 883. (g) Trost, B. M.; Shimizu, M. *J. Am. Chem. Soc.* **1982**, 104, 4299. (h) Ojima, I.; Yatabe, M.; Fuchikami, T. *J. Org. Chem.* **1982**, 47, 2051.
- (22) (a) Frankowski, K. J.; Golden, J. E.; Zeng, Y.; Lei, Y.; Aubé, J. *J. Am. Chem. Soc.* **2008**, 130, 6018. (b) Alonso, D.; Caballero, E.; Medarde, M.; Tomé, F. *Tetrahedron Lett.* **2007**, 48, 907. (c) Caballero, E.; Alonso, D.; Peláez, R.; Álvarez, C.; Puebla, P.; Sanz, F.; Medarde, M.; Tomé, F. *Tetrahedron* **2005**, 61, 6871. (d) Caballero, E.; Alonso, D.; Peláez, R.; Álvarez, C.; Puebla, P.; Sanz, F.; Medarde, M.; Tomé, F. *Tetrahedron Lett.* **2004**, 45, 1631.
- (23) (a) Nakashima, D.; Yamamoto, H. *J. Am. Chem. Soc.* **2006**, 128, 9626. (b) Ruijter, E.; Schültingkemper, H.; Wessjohann, L. A. *J. Org. Chem.* **2005**, 70, 2820. (c) Boezio, A. A.; Jarvo, E. R.; Lawrence, B. M.; Jacobsen, E. N. *Angew. Chem., Int. Ed.* **2005**, 44, 6046. (d) Chaplin, J. H.; Edwards, A. J.; Flynn, B. L. *Org. Biomol. Chem.* **2003**, 1, 1842. (e) Kraus, G. A.; Hon, Y. S.; Sy, J.; Raggon, J. *J. Org. Chem.* **1988**, 53, 1397. (f) Bell, V. L.; Holmes, A. B.; Hsu, S.-Y.; Mock, G. A.; Raphael, R. A. *J. Chem. Soc., Perkin Trans. 1* **1986**, 1507.

Table 1. Intermolecular Diels–Alder Reactions Involving Oxazolidinone Dienophiles

Entry	Reacting partners	Conditions	Major product	<i>exo/endo</i> <sup>a</sup>	Yield
1 <sup>b</sup>	<b>1a</b> + <b>3*</b>	1.4 equiv. Me <sub>2</sub> AlCl, CH <sub>2</sub> Cl <sub>2</sub> , -40 °C	 <i>endo-7</i>	1:5	50%
2 <sup>c</sup>	<b>1b</b> + <b>3*</b>		 <i>exo-8</i>	> 20:1	58%
3 <sup>d</sup>	<b>1c</b> + <b>3*</b>		 <i>exo-9</i>	> 20:1	65%
4 <sup>e</sup>	<b>2a</b> + <b>4</b>		 <i>endo-10<sup>f</sup></i>	1:20	78%
5	<b>2a</b> + <b>3</b>		 <i>exo-11</i>	> 20:1	62%
6	<b>2b</b> + <b>3</b>		 <i>exo-12</i>	> 20:1	89%
7	<b>2c</b> + <b>3</b>		 <i>exo-13</i>	> 20:1	80%
8	<b>2d</b> + <b>3*</b>		 <i>exo-14</i>	> 20:1	48%
9	<b>1a</b> + <b>5</b>	0.2–0.3 equiv. Me <sub>2</sub> AlCl, CH <sub>2</sub> Cl <sub>2</sub> , RT	 <i>endo-15</i>	1:4	15% <i>exo</i> 62% <i>endo</i>
10 <sup>c</sup>	<b>1b</b> + <b>6</b>		 <i>endo-16</i>	1:10	4% <i>exo</i> 40% <i>endo</i>
11 <sup>c</sup>	<b>1b</b> + <b>5</b>		 <i>exo-17</i>	11: (1:1.5:0.4) <sup>g</sup>	78% <i>exo</i>

<sup>a</sup> By 400 MHz <sup>1</sup>H NMR of the product mixture after aqueous workup. <sup>b</sup> Reference 20. <sup>c</sup> **1b** was used as an inseparable isomeric mixture with (*Z,E*)/(*E,E*) = 3:1. Reaction of only the major isomer was observed unless otherwise stated. <sup>d</sup> **1c** was used as a mixture with (*Z,E*)/(*E,E*) = 5:1. Reaction of only the major isomer was observed. <sup>e</sup> At -100 °C. <sup>f</sup> The product of protodesilylation of the primary endo cycloadduct, epimerized at C5, was isolated after chromatographic purification over silica gel. <sup>g</sup> Four sets of signals were observed by <sup>1</sup>H NMR of the crude mixture. Two of the adducts were assigned as *exo-17* and its C5 epimer. The other two minor adducts were tentatively assigned as the corresponding endo isomers.

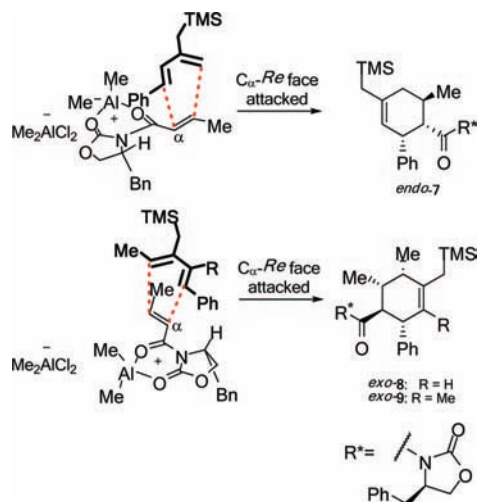


**Figure 2.** Rationalization of the sense of asymmetric induction in the **1a–c** + **3\*** cycloadditions.

asymmetric induction in both the endo- and exo-selective cycloadditions could be explained by Evans' model<sup>26</sup> (Figure 2). The oxazolidinone–Lewis acid complex is rigidified by chelation of both carbonyl groups to the aluminum. The benzyl group of the chiral auxiliary effectively shields the C<sub>α</sub>–Si face of the dienophile, giving rise to the sense of facial selectivity observed.

The same substituent-dependent variation in endo/exo selectivity was observed in the Diels–Alder reactions of 2-silyloxy-1,3-butadienes with **3** and **4**. Thus, the cycloaddition of diene **2a** and the achiral acryloyl oxazolidinone **4** was highly endo-selective (entry 4), while the same reaction with the crotonyl oxazolidinone **3** gave the exo cycloadduct **11** as the only product (entry 5). The stereoselectivity was not affected to any appreciable extent by changing either the silyl protecting group or the C4 substituent of the diene. The TIPS-protected silyloxydiene **2b** and the 1,4-dimethylsilyloxydiene **2c** respectively delivered *exo*-**12** (entry 6) and *exo*-**13** (entry 7) with high selectivity upon cycloaddition with **3**. The asymmetric cycloaddition of the silyloxydiene **2d** with **3\*** also yielded the expected product *exo*-**14** with high *exo/endo* and facial selectivities (entry 8). The high *exo* selectivity of asymmetric carbo Diels–Alder reactions using the auxiliary of **3\*** is rare in an intermolecular context.<sup>27</sup>

$\alpha,\beta$ -Unsaturated ketones were also studied with silylated dienes in the presence of catalytic Me<sub>2</sub>AlCl (entries 9–11). The same trend in endo/exo selectivity with substitution pattern was found. Thus, predominantly endo cycloaddition occurred when either C1 of the diene (entry 9) or the  $\beta$ -position of the dienophile (entry 10) was unsubstituted. For the combination

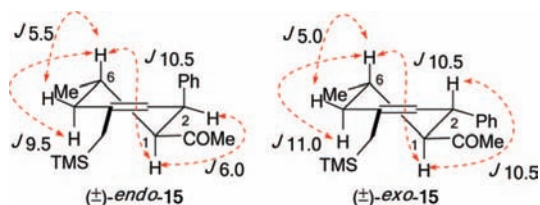


**Figure 3.** Key NMR coupling constants for stereochemical assignments, illustrated for *endo*- and *exo*-**15**.

of diene **1b** and dienophile **5**, each of which contained a terminal methyl group on the reacting double bonds, the reaction was *exo*-selective (entry 11).

The stereochemistries of all of the cycloadducts were readily assigned on the basis of proton NMR coupling constants (Figure 3) and confirmed in the case of *exo*-**8** by X-ray crystallography. In the *exo* cycloadducts, the signal due to the methine ring proton H1 (see Figure 1 for numbering) geminal to the carbonyl group appears as a triplet of ~10 Hz, consistent with vicinal coupling of H1 to two trans-diaxial protons (H2 and H6). In the *endo* counterparts with a C6 Me group (*endo*-**7**<sup>20</sup> and *endo*-**15**), this signal exists as a doublet of doublets with coupling constants of ~10 and 6 Hz, which respectively arise from one trans-diaxial pair and one axial–equatorial pair of coupled spins. The couplings of H1 in cycloadducts derived from acryloyl dienophiles (*endo*-**10** and *endo*-**16**) were also consistent with their stereochemistry.

Acyclic 2-silyloxy-1,3-butadienes substituted at one or both termini are useful dienes in Diels–Alder reactions directed toward a number of medically relevant targets. Despite their structural simplicity, the stereochemical outcomes observed with these substrates and cyclic dienophiles prove to be subtly dependent on the structure of the reactants and the Lewis acid.<sup>22,28</sup> The variation of the observed endo/exo selectivity with substitution pattern was rationalized in terms of steric clash between substituents on the approaching diene and dienophile. On the other hand, the use of oxazolidinone-containing dienophiles of the type **3\*** in R<sub>2</sub>AlCl-mediated Diels–Alder reactions is well-precedented for simple dienes, and the use of 2-silyloxydienes was documented recently.<sup>29</sup> We computationally investigated the transition states (TSs) of the current series of cycloadditions, focusing on how the substitution pattern of the starting material impacts the stereochemical outcome.

## Computational Methodology

Geometry optimizations and thermodynamic corrections were performed with hybrid density functional theory (B3LYP)<sup>30</sup> using the 6-31G(d)<sup>31</sup> basis set. MP2(default, frozen core)/6-31+G(d)//B3LYP/6-31G(d) single-point energies of endo and exo TSs were also computed and compared with the B3LYP-derived values and experimental data where available. Solvation corrections for the experimentally used solvent, dichloromethane, were calculated using

(24) (a) Narayanan, B. A.; Bunnelle, W. H. *Tetrahedron Lett.* **1987**, 28, 6261. (b) Hayashi, T.; Katsuro, Y.; Kumada, M. *Tetrahedron Lett.* **1980**, 21, 3915. (c) Yamamoto, Y.; Yamamoto, H. *Angew. Chem., Int. Ed.* **2005**, 44, 7082. (d) Kanemasa, S.; Kumegawa, M.; Wada, E.; Nomura, M. *Bull. Chem. Soc. Jpn.* **1991**, 64, 2990. Also see refs 20 and 23a.

(25) (a) Evans, D. A.; Chapman, K. T.; Bisaha, J. *J. Am. Chem. Soc.* **1984**, 106, 4261. (b) Thom, C.; Kocienski, P. *Synthesis* **1992**, 582. (c) Kanemasa, S.; Kanai, T. *J. Am. Chem. Soc.* **2000**, 122, 10710.

(26) Evans, D. A.; Chapman, K. T.; Bisaha, J. *J. Am. Chem. Soc.* **1988**, 110, 1238.

(27) For a recent example of the use of this chiral auxiliary in an *exo*-selective asymmetric hetero-Diels–Alder reaction, see: Evans, D. A.; Scheidt, K. A.; Downey, C. W. *Org. Lett.* **2001**, 3, 3009.

(28) (a) Zeng, Y.; Aubé, J. *J. Am. Chem. Soc.* **2005**, 127, 15712. (b) Zeng, Y.; Reddy, D. S.; Hirt, E.; Aubé, J. *Org. Lett.* **2004**, 6, 4993.

(29) Armstrong, A.; Davies, N. G. M.; Martin, N. G.; Rutherford, A. P. *Tetrahedron Lett.* **2003**, 44, 3915.

(30) (a) Becke, A. D. *J. Chem. Phys.* **1993**, 98, 1372. (b) Becke, A. D. *J. Chem. Phys.* **1993**, 98, 5648. (c) Lee, C.; Yang, W.; Parr, R. G. *Phys. Rev. B* **1988**, 37, 785.

(31) (a) Hehre, W. J.; Ditchfield, R.; Pople, J. A. *J. Chem. Phys.* **1972**, 56, 2257. (b) Hariharan, P. C.; Pople, J. A. *Theor. Chim. Acta* **1973**, 28, 213.

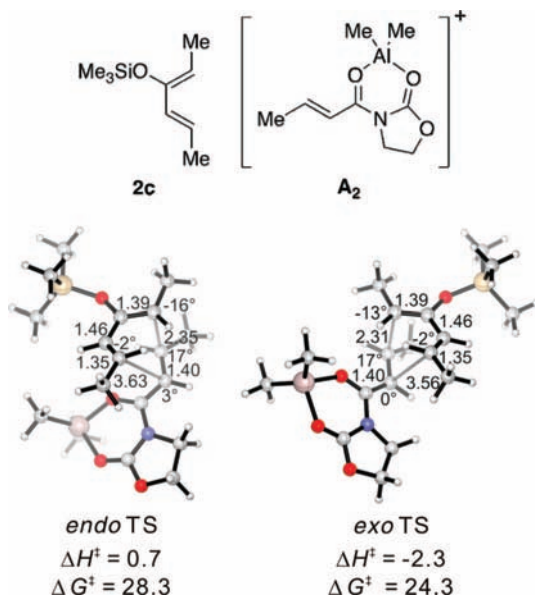


**Figure 4.** Endo and exo TSs of the  $2\mathbf{c} + \mathbf{A}_2$  cycloadditions. Gas-phase enthalpies of activation were computed at the B3LYP/6-31G(d) level, and free energies of activation were computed by B3LYP/6-31G(d) and corrected for solvent effects by PCM single-point calculations at the HF/6-31+G(d,p) level. Interatomic distances (Å) around the forming ring and angles of pyramidalization at the termini of the partially formed bonds are labeled.

the PCM method<sup>32</sup> and UAKS radii with single-point calculations at the HF/6-31+G(d,p) level of theory.<sup>33</sup>

Optimization of transition-structure geometries was started from a boatlike input structure expected from the general Diels–Alder reaction. The distance of the shorter of the forming bonds (C5–C6) was first held fixed and the remainder of the structure optimized. This distance constraint was then lifted, and the structure was reoptimized to the TS.<sup>34</sup> All of the energy minima and transition structures were characterized by frequency analysis.

All of the calculations were performed with *Gaussian 03*.<sup>35</sup>

## Computational Results and Discussion

We first computationally examined a Diels–Alder reaction involving the oxazolidinone-containing dienophile **3** for which experimental data were available. Dienophile **3** in the presence of  $\text{Me}_2\text{AlCl}$  was represented by the bidentate complex  $\mathbf{A}_2$  (Figure 4) in computations. Chiral complexes of the type  $\mathbf{A}_2$  have been invoked as the reactive species in  $\text{R}_2\text{AlCl}$ -mediated asymmetric Diels–Alder reactions<sup>26</sup> and have been characterized in solution by NMR.<sup>36</sup>

The  $\text{Me}_2\text{AlCl}$ -mediated cycloaddition of silyloxydiene **2c** and **3** was completely exo-selective (Table 1, entry 7). The endo and exo TSs of the  $2\mathbf{c} + \mathbf{A}_2$  addition are presented in Figure 4, which shows their boatlike geometries. B3LYP and second-order Møller–Plesset perturbation theory (MP2) calculations predict differences of 2.9 and 2.1 kcal/mol, respectively, in the electronic activation barriers ( $\Delta E^\ddagger$ ), both in favor of the exo pathway (Table 2). The difference in the free energies of activation ( $\Delta G^\ddagger$ ) for the endo and exo approaches, after correcting for solvent effects, is 4.0 kcal/mol (Figure 4). The experimental level and sense of diastereoselectivity was thus

**Table 2.** Activation Barriers and Their Dissection into Distortion and Interaction Energies (all in kcal/mol) for the Endo and Exo TSs of  $2\mathbf{c} + \mathbf{A}_2$

entry	method	pathway	$\Delta E^\ddagger$	$\Delta E_d^\ddagger$		$\Delta E_i^\ddagger$
				diene <b>2c</b>	dienophile complex $\mathbf{A}_2$	
1	B3LYP/ 6-31G(d)	endo	−0.1	9.5	11.9	−21.4
2		exo	−3.0	7.9	8.8	−19.7
3	MP2/ 6-31+G(d)	endo	−11.4	9.8	12.0	−33.1
4		exo	−13.5	8.3	8.8	−30.6

consistent with computation. The activation enthalpies ( $\Delta H^\ddagger$ ) refer to the difference between the enthalpy of the TS and the sum of enthalpies of the diene and the dienophile complex at infinite separation in the gas phase. The small, negative gas-phase  $\Delta H^\ddagger$  values (and the negative  $\Delta E^\ddagger$  values; see below) are often observed in modeling gas-phase ion/molecule reactions in general.<sup>37,38</sup> In the present case, they are consistent with the more favorable electrostatic attractions expected to exist between the diene's electrons and the cationic  $\mathbf{A}_2$  at the TS compared with the separate, unbound state.

Decomposition of the activation barrier  $\Delta E^\ddagger$  into a distortion energy ( $\Delta E_d^\ddagger$ ) and an interaction energy ( $\Delta E_i^\ddagger$ )<sup>37,39</sup> yields valuable insight into the difference between the activation energies of the endo and exo pathways. This analysis has previously been applied in understanding 1,3-dipolar and Diels–Alder cycloadditions.<sup>40</sup> The distortion energy is the energy required to distort the diene and the dienophile complex into the geometries they have at the TS without allowing interaction between them. The activation barrier is then the sum of the distortion and interaction energies:  $\Delta E^\ddagger = \Delta E_d^\ddagger + \Delta E_i^\ddagger$ , where the interaction energy term encompasses all of the stabilizing and repulsive interactions between the diene and dienophile fragments at the TS. Table 2 lists the activation barriers and distortion and interaction energies for the endo and exo Diels–Alder TSs of  $2\mathbf{c} + \mathbf{A}_2$ , computed using the B3LYP and MP2 methods.

The distortion energy values calculated using B3LYP or MP2 are very similar in most cases, but MP2 predicts that the interactions at the endo TS are more stabilizing than those at the exo TS by a larger margin than B3LYP does. MP2 favors the endo pathway to a greater extent than B3LYP for all of the investigated cycloadditions. The underestimation of endo/exo selectivity by B3LYP due to problems in describing long-range dispersion interactions has been noted.<sup>41,42</sup>

It is noteworthy that the interactions between the diene and dienophile fragments are more stabilizing at the endo TS than at the exo TS, regardless of the computational method used. The net preference for exo selectivity observed in  $2\mathbf{c} + \mathbf{A}_2$  is therefore the result of more severe reactant distortions that overwhelm the more favorable interaction energies in the endo TS. The geometries of reactants **2c** and  $\mathbf{A}_2$  in their cycloaddition

(32) Tomasi, J.; Persico, M. *Chem. Rev.* **1994**, *94*, 2027.

(33) Takano, Y.; Houk, K. N. *J. Chem. Theory Comput.* **2005**, *1*, 70.

(34) Birney, D. M.; Houk, K. N. *J. Am. Chem. Soc.* **1990**, *112*, 4127.

(35) Frisch, M. J.; et al. *Gaussian 03*, revisions C.02 and D.01; Gaussian, Inc.: Wallingford, CT, 2004.

(36) Castellino, S.; Dwight, W. J. *J. Am. Chem. Soc.* **1993**, *115*, 2986.

(37) Bickelhaupt, F. M. *J. Comput. Chem.* **1999**, *20*, 114.

(38) DeChancie, J.; Acevedo, O.; Evansck, J. D. *J. Am. Chem. Soc.* **2004**, *126*, 6043.

(39) Nagase, S.; Morokuma, K. *J. Am. Chem. Soc.* **1978**, *100*, 1666.

(40) (a) Ess, D. H.; Houk, K. N. *J. Am. Chem. Soc.* **2008**, *130*, 10187. (b) Ess, D. H.; Houk, K. N. *J. Am. Chem. Soc.* **2007**, *129*, 10646. (c) Ess, D. H.; Jones, G. O.; Houk, K. N. *Org. Lett.* **2008**, *10*, 1633. (d) García, J. I.; Martínez-Merino, V.; Mayoral, J. A.; Salvatella, L. *J. Am. Chem. Soc.* **1998**, *120*, 2415. (e) Sbai, A.; Branchadell, V.; Ortuño, R. M.; Oliva, A. *J. Org. Chem.* **1997**, *62*, 3049.

(41) Wannere, C. S.; Paul, A.; Herges, R.; Houk, K. N.; Schaefer, H. F., III; Schleyer, P. v. R. *J. Comput. Chem.* **2007**, *28*, 344.

(42) Tsuzuki, S.; Lüthi, H. P. *J. Chem. Phys.* **2001**, *114*, 3949.

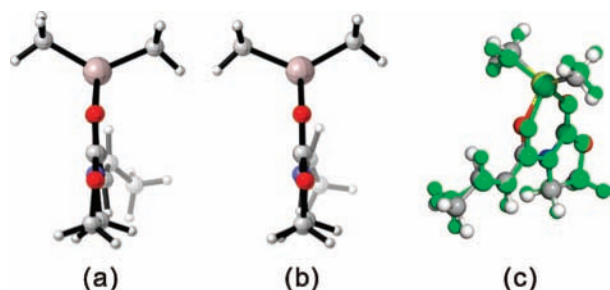


**Figure 5.** Side view of the  $A_2$  dienophile fragment in the (a) endo and (b) exo  $2c + A_2$  TSs. (c) Overlay of the  $A_2$  dienophile fragments in the two TSs of  $2c + A_2$  (green atoms, endo; other-colored atoms, exo).

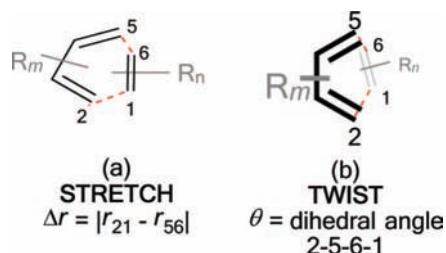


**Figure 6.** Schematic illustration of the two modes of asynchronicity at the TS of a Diels–Alder reaction.

TS geometries provide an illustrative example of reactant distortions (Table 2). The diene fragment is more heavily deformed at the endo TS by  $\sim 1.5$  kcal/mol, and the dienophile is distorted twice as much (3.1 kcal/mol). The origin of the dramatic difference in distortion energies of  $A_2$  in the two TSs is most easily visualized by a side-on view of the dienophile complex, as shown in Figure 5. The methyl group of dienophile  $A_2$  is bent out of the olefinic plane more severely in the endo TS ( $25^\circ$ , Figure 5a) than in the exo TS ( $14^\circ$ , Figure 5b), indicating that it suffers greater repulsion from the vicinal diene methyl group in the endo TS.

A twist-asynchronous model shows how vicinal disubstitution can lead to a large distortion in the endo TS, which is chiefly responsible for the exo selectivity found computationally and experimentally.

In general, Diels–Alder reactions of unsymmetrical dienes and dienophiles proceed through concerted<sup>43</sup> asynchronous<sup>44</sup> mechanisms.<sup>45</sup> Two modes of asynchronicity in Diels–Alder reactions can be distinguished (Figure 6). The stretch mode refers to the differing lengths of the two forming C–C bonds at the transition state (Figure 6a). The twist mode refers to the deviation of the diene and the dienophile backbones from being parallel and can be measured by a twist-asynchronicity parameter,  $\theta$ , given by the C2–C5–C6–C1 dihedral angle, where C5–C6 is the shorter of the forming C–C bonds (Figure 6b). The impact of catalyst coordination on stretch-mode asynchronicity of Diels–Alder reactions has been well-discussed.<sup>46</sup> A

twist-asynchronous model was first put forward by Brown and Houk<sup>47</sup> to account for substituent-induced selectivity variation in the context of intramolecular Diels–Alder (IMDA) reactions. This has seen extensive application in the rationalization of stereoselectivity in the IMDA reactions of other substrates.<sup>48</sup>

Table 3 lists the endo and exo TSs for the Diels–Alder reactions of a series of silyloxydienes and other model dienes with the oxazolidinone-bearing dienophile **3**, either in the presence of  $Me_2AlCl$  (represented by the dienophile complex  $A_2$ ) or in its absence. These are presented as Newman projections along the shorter of the forming bonds (C5–C6).

It is clear from Table 3 that the endo series of TSs displays a wider range of twist-mode asynchronicities than the exo TSs. Depending on diene substitution,  $\theta$  varies from  $+12$  to  $-33^\circ$  for the endo TSs and from  $+10$  to  $+23^\circ$  for the exo TSs. The endo TS of the exo-selective  $2c + A_2$  cycloaddition is highly twisted, with  $\theta = -33^\circ$ , and features a very small Me–Me dihedral angle of  $23^\circ$  (entry 1). The corresponding exo TS is much less twisted and places the vicinal Me groups at a dihedral angle of  $72^\circ$ . The large difference in the Me–Me dihedral angles of the two TSs explains why the dienophile complex experiences a higher distortion at the endo TS.

Replacing the C1 methyl group of **2c** with hydrogen, resulting in the desmethyl diene **2e**, reduces the allylic 1,3-strain across the silyl enol ether and allows TSs containing the s-syn rotamer of **2e** to be located. These TSs, which are displayed in entry 2, are more stable than the corresponding TSs containing the s-anti conformer of **2e**. The levels of twisting are smaller, leading to similar H–Me dihedral angles in the two TSs, concomitant with a much smaller relative stability of the exo TS. MP2 even predicts that the endo TS is more stable. The TS geometries and energies are therefore heavily affected by the C1 methyl substituent in this system.

What causes the drastic asynchronous twist in the endo  $2c + A_2$  TS? To assess its origin, we modeled the TSs involving diene **2f**, in which a methoxy group replaces the silyloxy group in **2c** (entry 3). The computed free energies of activation indicate that as a result of this replacement, the exo/endo difference decreases from 4.0 kcal/mol (entry 1) to 2.3 kcal/mol (entry 3). The endo TS is also less twisted, with  $\theta = -13^\circ$ , placing the vicinal Me groups at a dihedral angle of  $44^\circ$ . The twist-asynchronicity and the resultant Me–Me dihedral angle are practically the same in the exo TSs involving either the methoxy or the silyloxy diene. Since the methoxy and trimethylsilyloxy groups can be expected to possess similar electronic properties (both dominated by oxygen), steric interactions, plausibly between the trimethylsilyloxy group and the dimethylaluminum portion of  $A_2$ , are one contributor to the high twist-asynchronicity in the endo  $2c + A_2$  TS. Another destabilizing factor is electrostatic repulsion between the oxygenated group and the aluminum-bound dienophile. As the TSs of  $2c + 3$  (entry 4) show, the asynchronous twist is considerably less severe in the absence of the Lewis acid, resulting in the more typical Me–Me

(43) (a) Goldstein, E.; Beno, B.; Houk, K. N. *J. Am. Chem. Soc.* **1996**, *118*, 6036. (b) Storer, J. W.; Raimondi, L.; Houk, K. N. *J. Am. Chem. Soc.* **1994**, *116*, 9675. (c) Houk, K. N.; Lin, Y. T.; Brown, F. K. *J. Am. Chem. Soc.* **1986**, *108*, 554.

(44) (a) Singleton, D. A.; Schulmeier, B. E.; Hang, C.; Thomas, A. A.; Leung, S.-W.; Merrigan, S. R. *Tetrahedron* **2001**, *57*, 5149. (b) Beno, B. R.; Houk, K. N.; Singleton, D. A. *J. Am. Chem. Soc.* **1996**, *118*, 9984.

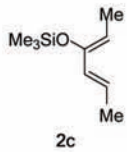
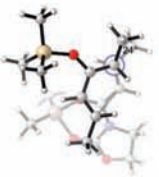
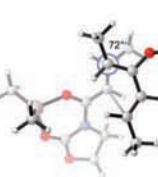
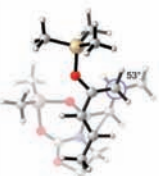
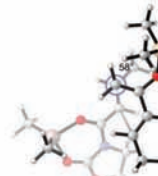
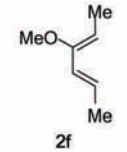
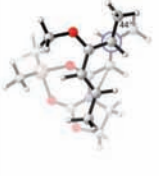
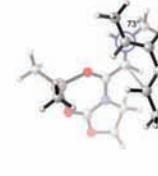
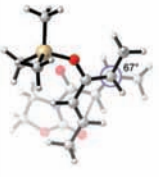
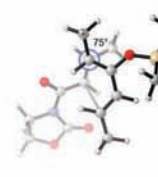
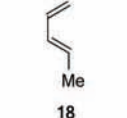
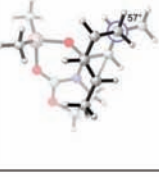
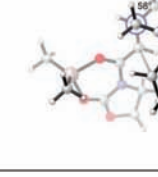
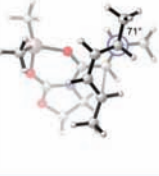
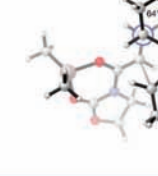
(45) Houk, K. N.; Gonzalez, J.; Li, Y. *Acc. Chem. Res.* **1995**, *28*, 81. For an up-to-date discussion of Diels–Alder mechanisms, also see: Bachrach, S. M. *Computational Organic Chemistry*; Wiley: Hoboken, NJ, 2007; pp 128–133.

(46) García, J. I.; Mayoral, J. A.; Salvatella, L. *J. Am. Chem. Soc.* **1996**, *118*, 11680. Also see refs 34 and 40d,e.

(47) (a) Brown, F. K.; Houk, K. N. *Tetrahedron Lett.* **1985**, *26*, 2297. (b) Wu, T.-C.; Houk, K. N. *Tetrahedron Lett.* **1985**, *26*, 2293.

(48) (a) Tripoli, R.; Cayzer, T. N.; Willis, A. C.; Sherburn, M. S.; Paddon-Row, M. N. *Org. Biomol. Chem.* **2007**, *5*, 2606. (b) Paddon-Row, M. N.; Moran, D.; Jones, G. A.; Sherburn, M. S. *J. Org. Chem.* **2005**, *70*, 10841. (c) Cayzer, T. N.; Paddon-Row, M. N.; Moran, D.; Payne, A. D.; Sherburn, M. S.; Turner, P. *J. Org. Chem.* **2005**, *70*, 5561. (d) Lilly, M. J.; Paddon-Row, M. N.; Sherburn, M. S.; Turner, C. I. *Chem. Commun.* **2000**, 2213.

**Table 3.** Endo (n) and Exo (x) TS Geometries and Energetics (kcal/mol) for a Range of Silyloxydienes and Other Model Dienes with Dienophile Complex **A**<sub>2</sub> or Dienophile **3**, with an Emphasis on Twist-Mode Asynchronicity

entry	diene	TS geometry		$\Delta G_{298}^{\ddagger a}$	$\Delta E_0^{\ddagger b}$	$\theta^c$	Me(H)–Me dihedral angle
		<i>endo</i>	<i>exo</i>				
1	 2c			28.3(n) 24.3(x)	−0.1 (−11.4) (n) −3.0 (−13.5) (x)	−33° (n) +22° (x)	24°(n) 72°(x)
				24.1(n) 24.0(x)	−2.0 (−13.1) (n) −2.1 (−11.4) (x)	−5° (n) +10° (x)	53°(n) 58°(x)
3	 2f			25.9(n) 23.6(x)	0.4 (−11.0) (n) −1.7 (−11.4) (x)	−13° (n) +23° (x)	44°(n) 73°(x)
				42.7(n) 40.1(x)	21.0 (4.5) (n) 20.2 (5.6) (x)	+9° (n) +23° (x)	67°(n) 75°(x)
5	 18			28.9(n) 29.6(x)	6.9 (−3.8) (n) 7.3 (−2.1) (x)	−3° (n) +12° (x)	57°(n) 58°(x)
				34.7(n) 33.3(x)	10.6 (−4.2) (n) 9.1 (−4.5) (x)	+12° (n) +16° (x)	71°(n) 64°(x)

<sup>a</sup> Gas-phase Gibbs free energy of activation at B3LYP/6-31G(d) level, corrected for solvent effects by PCM single-point calculations at the HF/6-31+G(d,p) level on B3LYP/6-31G(d) vacuum-optimized geometries. <sup>b</sup> Gas-phase uncorrected electronic energy at the B3LYP/6-31G(d)//B3LYP/6-31G(d) level. The corresponding energy at the MP2/6-31+G(d)//B3LYP/6-31G(d) level is given in parentheses. <sup>c</sup> Twist-asynchronicity parameter. See Figure 6b for definition. <sup>d</sup> In the absence of Me<sub>2</sub>AlCl (i.e., with dienophile **3**).

dihedral angles of 67° (endo) and 75° (exo). The exo preference is again diminished, and the MP2 energies even indicate an endo

preference. Electrostatic repulsion between the lone pair on a heterodienophile and the diene is well-known to influence



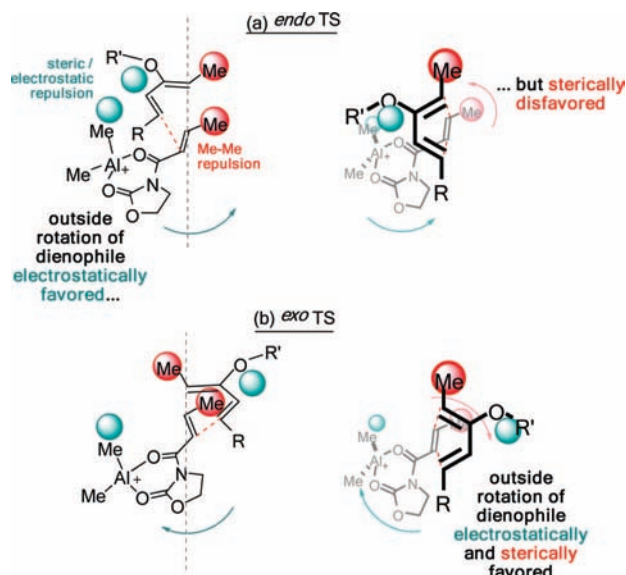


**Figure 7.** Twist-asynchronicity model delineating the origin of exo selectivity in Diels–Alder reactions involving oxygenated dienes.

stereochemical preferences<sup>49</sup> and dictate reaction trajectories<sup>50</sup> of hetero-Diels–Alder reactions. Analogous interactions should also operate in the *endo* **2c** + **A**<sub>2</sub> system.

On the basis of the above discussion, a twist-asynchronous model rationalizing the substituent effects on the relative *endo* and *exo* TS energies in the Diels–Alder reactions of silyloxydienes is presented in Figure 7. In the *endo* series of TSs (Figure 7a), steric and electrostatic interactions between the diene C2 substituent and the aluminum-complexed dienophile drives the rotation of the latter in the outward direction. This motion is disfavored when both ends of the shorter of the forming bonds (C5–C6) are methyl-substituted, since the rotation brings them close together and aggravates the vicinal repulsion between them. The twist-asynchronicity of these TSs reflects the tradeoff between the two types of repulsion arising from their respective local environments within the TSs. In contrast, the *exo* TSs are less prone to these destabilizing interactions. As Figure 7b shows, the twisting that would alleviate the steric and electrostatic interactions also moves any vicinal methyl substituents on the forming C5–C6 bond further apart. The *exo* series of TSs could therefore relax by asynchronous twisting as appropriate. Indeed, when the 2-silyloxy- or 2-methoxydiene is methyl-substituted at both termini, the *exo* TSs consistently displays a narrow range of Me–Me dihedral angles between 69 and 75° (Table 3, entries 1, 3, and 4). This model explains why the relative energies of the *endo* and the *exo* TSs for a given cycloaddition depend heavily on the substitution pattern and why the *exo* TS is, in most cases, less destabilized than the *endo* TS.

Computations of Diels–Alder TSs of the dienophile complex **A**<sub>2</sub> with a series of structurally simpler dienes give further support to the twist-asynchronicity model. *trans*-Piperylene (**18**) was reported by Evans et al.<sup>26</sup> to react with **3\*** in the presence of Et<sub>2</sub>AlCl with an *endo/exo* selectivity superior to 95:5. Modeling of the TSs of the **18** + **A**<sub>2</sub> addition (Table 3, entry 5), with MP2 single-point energies, reproduced the experimental

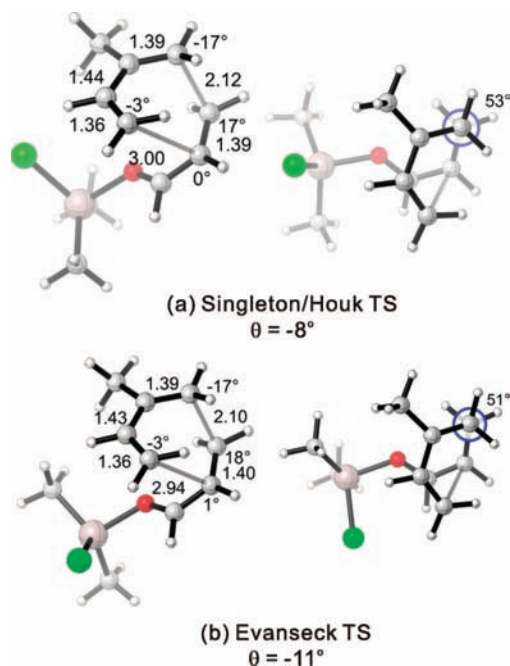


**Figure 8.** B3LYP/6-31G(d) *endo* TSs for the reaction of isoprene with acrolein·AlMe<sub>2</sub>Cl obtained by (a) Singleton/Houk and (b) Evanseck.

level and sense of the *endo/exo* selectivity. The twisting of these TSs is small and comparable to that of the TSs involving the 2-trimethylsilyloxydiene **2e** (entry 2). The substituents around the shorter of the forming C–C bonds are arranged in an approximately staggered manner. The low level of twisting of the *endo* **18** + **A**<sub>2</sub> TS could be favorably compared to that of the TSs computed in the dialkylaluminum chloride-catalyzed Diels–Alder reaction of isoprene and acrolein. Singleton, Houk, and co-workers<sup>51</sup> and Acevedo and Evanseck<sup>52</sup> have shown that the TS of this reaction, which was validated by experimental and calculated kinetic isotope effects, corresponds to the *endo* approach of the two reactants. The computed TSs (Figure 8) display a low level of asynchronous twist and a nearly staggered arrangement of substituents around the shorter of the forming C–C bonds, similar to the *endo* **18** + **A**<sub>2</sub> TS. Consequently, the greater stabilization of the *endo* TSs determines the stereoselectivity.

Adding a terminal methyl substituent to *trans*-piperylene gives 2,4-hexadiene (**19**). *Exo* selectivity is now found (Table 3, entry 6). In the *endo* TS, the backbones of the diene and the dienophile are skewed, with  $\theta = +12^\circ$ . The Me–Me repulsion forces the dienophile away from ideal overlap with the remote terminus of the diene. Although the *endo* TS is now more destabilized (according to B3LYP energies), the magnitude of such destabilization is small (a 1.4 kcal/mol free-energy difference) compared with the cases where the diene is additionally substituted at the 2-position (2–4 kcal/mol, Table 3, entries 1 and 3). The “back side” of the *endo* **19** + **A**<sub>2</sub> TS is not hindered by substituents. This allows the dienophile to rotate inward to alleviate the vicinal dimethyl repulsion and the accompanying destabilization.

The phenyl-substituted silylated dienes **1b** and **1a** used in the experimental studies were modeled by the methyl analogs

(49) Iafe, R. G.; Houk, K. N. *J. Org. Chem.* **2008**, *73*, 2679.

(50) (a) Leach, A. G.; Houk, K. N. *J. Org. Chem.* **2001**, *66*, 5192. (b) McCarrick, M. A.; Wu, Y. D.; Houk, K. N. *J. Org. Chem.* **1993**, *58*, 3330.

(51) Singleton, D. A.; Merrigan, S. R.; Beno, B. R.; Houk, K. N. *Tetrahedron Lett.* **1999**, *40*, 5817.

(52) Acevedo, O.; Evanseck, J. D. *Org. Lett.* **2003**, *5*, 649.

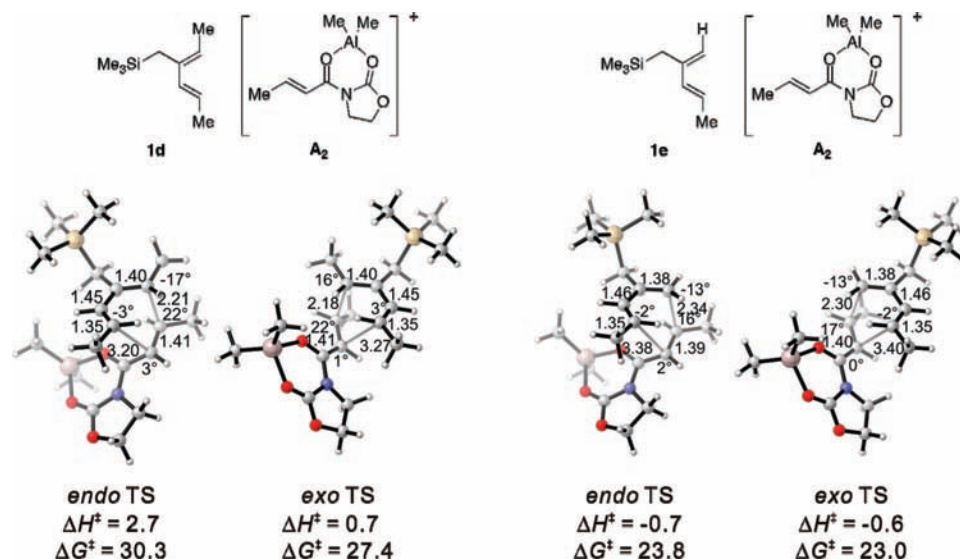


**Figure 9.** Endo and exo TSs of the **1d** + **A<sub>2</sub>** and **1e** + **A<sub>2</sub>** cycloadditions. Gas-phase enthalpies of activation were computed at the B3LYP/6-31G(d) level, and free energies of activation were computed by B3LYP/6-31G(d) and corrected for solvent effects by PCM single-point calculations at the HF/6-31+G(d,p) level. Interatomic distances (Å) around the forming ring and angles of pyramidalization at the termini of the partially formed bonds are labeled.

**Table 4.** Activation Barriers and Their Dissection into Distortion and Interaction Energies (all in kcal/mol) for the Endo and Exo TSs of **1d** + **A<sub>2</sub>** and **1e** + **A<sub>2</sub>**

entry	reactants	method	pathway	$\Delta E^\ddagger$	$\Delta E_d^\ddagger$		$\Delta E_i^\ddagger$
					diene	dienophile complex <b>A<sub>2</sub></b>	
1	<b>1d</b> + <b>A<sub>2</sub></b>	B3LYP/6-31G(d)	endo	2.0	10.9	14.2	-23.2
2			exo	-0.1	9.2	12.7	-22.0
3		MP2/6-31+G(d)	endo	-14.8	10.0	14.3	-39.1
4			exo	-14.1	8.4	12.7	-35.2
5	<b>1e</b> + <b>A<sub>2</sub></b>	B3LYP/6-31G(d)	endo	-1.4	6.0	7.6	-15.0
6			exo	-1.3	6.3	8.2	-15.8
7		MP2/6-31+G(d)	endo	-12.9	5.9	7.6	-26.3
8			exo	-11.2	6.1	8.2	-25.4

**1d** and **1e**, respectively. The free energies of activation of their cycloadditions with **A<sub>2</sub>** indicate that the exo preference is very strong in the case of diene **1d** and much diminished for diene **1e**, where the C1 methyl group on the diene is replaced by hydrogen (Figure 9). This trend is consistent with the experimental results for the cycloadditions of **3\*** with **1a** and **1b** (Table 1, entries 1 and 2). The moderate endo selectivity in the experimental **1a** + **3\*** reaction could not be reproduced by the B3LYP energies of the **1e** + **A<sub>2</sub>** TSs, although the MP2 single-point energies predicted a much higher proportion of the endo product. MP2 methods have been shown in some cases to be more accurate in reproducing experimental trends, particularly when weak nonbonding interactions are involved.<sup>5,41,53</sup>

An analysis of the distortion and interaction energies (Table 4) shows that the distortion energies in the endo TS again overwhelm the more favorable interaction energies in the presence of vicinal disubstitution, accounting for the observed exo preference. The sum of the distortion energies of the diene

**1d** and dienophile complex **A<sub>2</sub>** is 3.2 kcal/mol higher in the endo TS than in the exo TS, while the corresponding difference involving the desmethyl analog **1e** favors the endo pathway by only ~0.9 kcal/mol.

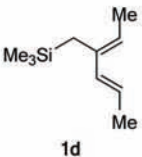
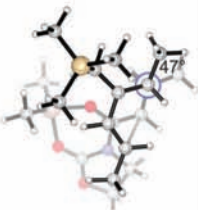
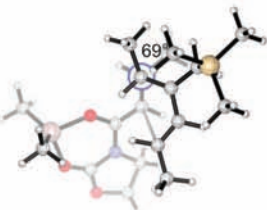
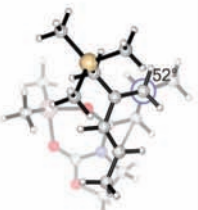
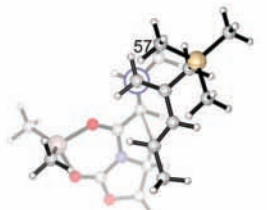
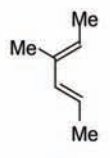
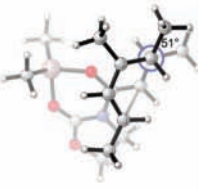
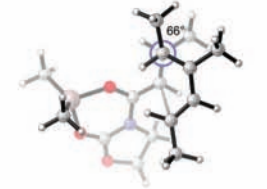
Replacing the oxygen in **2c** and **2e** with methylene, giving the all-carbon silylated dienes **1d** and **1e**, respectively, leads to considerable alleviation of the twisting in both the endo and exo TSs with **A<sub>2</sub>** (Table 5, entries 1 and 2). These TSs display  $\theta$  values between  $-6$  and  $-15^\circ$ . This is consistent with the reduction of electrostatic repulsion between the diene and dienophile fragments as a result of this replacement. To investigate the influence of the silyl functionality, we computed model TSs for the reaction of **A<sub>2</sub>** with 3-methylhexa-2,4-diene (**20**), in which the silyl group is replaced by a hydrogen (Table 5, entry 3). For the **20** + **A<sub>2</sub>** addition, a difference of 1.4 kcal/mol in the free energies of activation favoring the exo product was computed; this is the same in magnitude and direction as that involving the C2-desmethyl diene **19** (Table 3, entry 6) but only half of that observed for the corresponding silylated diene **1d** (Table 5, entry 1). The C2 methyl substituent on the diene does perturb the endo TS geometry, as the vicinal methyl groups are now set at a dihedral angle of  $51^\circ$  compared with  $71^\circ$  in its absence. The change in the exo TS geometry is negligible. An extra trimethylsilyl group on the diene, however, causes little perturbation in the geometry of either the endo or the exo TS in terms of twist-mode asynchronicity and vicinal Me–Me dihedral angles in **1d** + **A<sub>2</sub>**. The amplified exo selectivity caused by the presence of the silyl group is likely to be electronic rather than steric in origin, although the precise underpinnings are more subtle in these cases.

## Conclusion

A new series of substituent-dependent exo-selective Diels–Alder reactions involving silylated dienes or silyloxydienes and  $\alpha,\beta$ -unsaturated *N*-acyloxazolidinone or ketone dienophiles has been studied experimentally and computationally. These reactions demonstrate the maximal stereochemical efficiency of the Diels–Alder reaction by installing four contiguous stereocenters in the cycloadduct with a very favorable exo selectivity and

(53) (a) Dinadayalane, T. C.; Vijaya, R.; Smitha, A.; Sastry, G. N. *J. Phys. Chem. A* **2002**, *106*, 1627. (b) Baki, S.; Maddaluno, J.; Derdour, A.; Chaquin, P. *Eur. J. Org. Chem.* **2008**, 3200. (c) Bakalova, S. M.; Santos, A. G. *J. Org. Chem.* **2004**, *69*, 8475. (d) Bakalova, S. M.; Kaneti, J. *J. Phys. Chem. A* **2008**, *112*, 13006.

**Table 5.** Endo (n) and Exo (x) TS Geometries and Energetics (kcal/mol) for a Range of Substituted Silylated Dienes and a Model Diene with Dienophile Complex **A**<sub>2</sub>, with an Emphasis on Twist-Mode Asynchronicity

entry	diene	TS geometry		$\Delta G_{298}^{\ddagger a}$	$\Delta E_0^{\ddagger b}$	$\theta^c$	Me(H)–Me dihedral angle
		<i>endo</i>	<i>exo</i>				
1	 1d	 47°	 69°	30.3(n) 27.4(x)	2.0 (–14.8) (n) –0.1 (–14.1) (x)	–6° (n) +15° (x)	47°(n) 69°(x)
		 52°	 57°	23.8(n) 23.0(x)	–1.4 (–12.9) (n) –1.3 (–11.2) (x)	–6° (n) +8° (x)	52°(n) 57°(x)
3	 20	 51°	 66°	31.3(n) 29.9(x)	6.8 (–9.8) (n) 5.5 (–9.4) (x)	–4° (n) +13° (x)	51°(n) 66°(x)

<sup>a</sup> Gas-phase Gibbs free energy of activation at the B3LYP/6-31G(d) level, corrected for solvent effects by PCM single-point calculations at the HF/6-31+G(d,p) level on the B3LYP/6-31G(d) vacuum-optimized geometries. <sup>b</sup> Gas-phase uncorrected electronic energy at the B3LYP/6-31G(d)//B3LYP/6-31G(d) level. The corresponding energy at the MP2/6-31+G(d)//B3LYP/6-31G(d) level is given in parentheses. <sup>c</sup> Twist-asynchronicity parameter. See Figure 6b for definition.

$\pi$ -facial selectivity. A systematic experimental study identified the structural prerequisites in the starting materials for such a high level of exo preference, namely, simultaneous methyl substitution on the diene and dienophile termini involved in the shorter of the forming C–C bonds. On the basis of computational investigations of both experimental and other model systems, a twist-mode asynchronicity model for understanding the origin of the endo/exo stereocontrol was put forward. Specifically, this work showed how the vicinal disubstituent effect could destabilize the highly asynchronous endo TSs, requiring rotations that reduce steric and electrostatic repulsion within the TSs at the expense of reactant distortion. Interaction energies favor the endo pathway, but this is overwhelmed by distortion that relieves gauche-type Me–Me repulsions. This work has moved us closer to a more comprehensive understanding of the factors controlling Diels–Alder endo/exo stereoselectivity. It should also contribute to more effective experimental planning in using this reaction in the stereodefined synthesis of many molecular targets featuring six-membered rings.

**Acknowledgment.** We thank Dr. Andrew Cowley for assistance with X-ray structure determination. This work was funded by the Croucher Foundation, Hong Kong (Y.-h.L.), the U.K. Overseas Research Studentship (Y.-h.L.), GlaxoSmithKline (Y.-h.L.), the U.K. Engineering and Physical Sciences Research Council (J.M.B.M.), and the National Institute of General Medical Sciences, National Institutes of Health (P.H.-Y.C., K.N.H.). Computational resources were provided by Academic Technology Services, UCLA, and the National Service for Computational Chemistry Software, EPSRC.

**Supporting Information Available:** Complete ref 35; crystallographic data for *exo*-**8** in CIF format; full experimental procedures and characterization data for all new compounds; and Cartesian coordinates, energies, and thermal corrections for all of the optimized reactants and transition structures. This material is available free of charge via the Internet at <http://pubs.acs.org>.

JA8079548